Nikita N. Harmalkar, Bikshandarkoil R. Srinivasan and Sunder N. Dhuri*

Synthesis, structure characterization and properties of a new oxidovanadium(IV) coordination polymer incorporating bridging $(MoO_4)^{2-}$ and $(Mo_8O_{26})^{4-}$ ligands

https://doi.org/10.1515/znb-2022-0005
Received January 13, 2022; accepted January 20, 2022;
published online February 4, 2022

Abstract: Hydrothermal synthesis, crystal structure and properties of a new heterometallic coordination polymer $[(VO(terpy))_4(MoO_4)_2(Mo_8O_{26})]\cdot 2H_2O$ (**1**) (terpy = 2,2′;6′,2″-terpyridine) are reported. Compound **1** contains two crystallographically unique vanadium(IV) atoms, bonded to a terminal oxido ligand and further coordinated to a terpy ligand. The three N atoms of terpy occupy the meridional sites of a distorted $\{VN_3O_3\}$ octahedron. A γ-octamolybdate $(Mo_8O_{26})^{4-}$ located on an inversion centre and a tetraoxidomolybdate $(MoO_4)^{2-}$ function as bridging ligands. The μ_3-bridging tridentate binding of $(MoO_4)^{2-}$ leads to the formation of a $\{V_4Mo_2O_{12}\}^{4+}$ cationic unit consisting of an eight-membered heterometallic $\{Mo_2V_2O_4\}$ ring with protruding oxidovanadium handles. A pair of $\{V_4Mo_2O_{12}\}^{4+}$ units are bridged by the centrosymmetric $(Mo_8O_{26})^{4-}$ ligand, resulting in the formation of an infinite chain of alternating $\{V_4Mo_2O_{12}\}^{4+}$ cations and $(Mo_8O_{26})^{4-}$ anions.

Keywords: γ-octamolybdate; bridging ligand; coordination polymer; tetraoxidomolybdate; vanadium.

Dedicated to Professor Christian Näther on the occasion of his 60th birthday.

1 Introduction

Polyoxometalates (POMs) are discrete anionic transition metal clusters having unique topologies, nuclearities and electronic versatilities. The isopoly- and heteropolyanion clusters usually contain symmetrical core assemblies of metal-oxido motifs (M = V, Mo, W) and often adopt quasi-spherical structures of considerable topological interest [1, 2]. POMs are formed in condensation processes of simple anions in solution under different temperature and pH (mainly acidic) conditions [3, 4]. Due to their promising biological applications [5, 6] POMs are actively used as metallodrugs. In recent years, they are gaining importance for their antitumor, antiviral, antibacterial, anticancer activities [6]. In addition, these compounds exhibit remarkable redox properties and thus find potential applications in several areas viz. catalysis, medicine, electrochemistry, magnetic materials etc. [7–12]. The concept of hybrid polyoxometalates has emerged in recent years. These post-functionalizable hybrid-POMs serve as building blocks due to structural diversity in such a way that they allow coupling of properties of POMs with different organic and inorganic metal cation functionalities making them useful in (photo) catalysis, bioinorganic chemistry and material science [13, 14]. The structural, electronic and magnetic properties of well-known polyoxovanadates (POVs), such as the robust $[V^{IV}_{18}O_{42}]^{12-}$ polyoxoanion can be altered by replacement of V by elements like Si-, Ge-, As- or Sb to form decorated heteroPOVs. The four general families of POVs are: fully-oxidised (V^V), mixed-valent (V^V/V^{IV} or V^{IV}/V^{III}), "fully-reduced" (V^{IV}) and "highly-reduced" (V^{III}) species [15–17].

The chemistry of POVs is dominated by the decavanadate anion $[V_{10}O_{28}]^{6-}$ containing the fully oxidised V^V ion [18–20] and several examples of structurally characterized decavanadates charge balanced by a variety of counter cations are listed in the Cambridge Structural Database [21]. As in the case of other early transition metals like Mo and W [22, 23], decavanadates can be readily obtained by treatment of V_2O_5 with a limited amount of base [24] or by acidification of tetraoxidovanadate/metavanadate solution in the presence of appropriate counter cations [25–28]. Unlike decavanadates, the fully reduced POVs containing V^{IV} are air-sensitive as evidenced by the report on the Na^+ or K^+ salt of $[V^{IV}_{18}O_{42}]^{12-}$ [29]. In this spherical polyoxoanion each of the eighteen V^{4+} cations is coordinated by five oxygen atoms, one of which is unshared

***Corresponding author: Sunder N. Dhuri**, School of Chemical Sciences, Goa University, Goa 403206, India,
E-mail: sndhuri@unigoa.ac.in. https://orcid.org/0000-0003-2732-880X
Nikita N. Harmalkar and Bikshandarkoil R. Srinivasan, School of Chemical Sciences, Goa University, Goa 403206, India. https://orcid.org/0000-0002-6598-6726 (B.R. Srinivasan)

pointing outwards of the cluster shell, which is a typical structural feature in the chemistry of the vanadyl $[VO]^{2+}$ moiety. The stringent air-free conditions required to access V^{4+} species in aqueous chemistry can be overcome in hydrothermal reactions by use of a N-donor ligand as structure directing agent as evidenced by the synthesis of the heterometallic compounds $[VO(\eta^1\text{-}MoO_4)(tren)]\cdot H_2O$ (tren = tris-2-aminoethylamine), $[VO(\mu_3\text{-}MoO_4)(bpy)]$ (bpy = 2,2′-bipyridine) etc. [30–32]. During the course of our investigations aimed at the synthesis of mixed metal hybrid organic compounds, we obtained a new heterometallic coordination polymer $[(VO(terpy))_4(MoO_4)_2(Mo_8O_{26})]\cdot 2H_2O$ (**1**), (terpy = 2,2′;6′,2″-terpyridine) containing bridging γ-octamolybdate $(Mo_8O_{26})^{4-}$ and tetraoxidomolybdate $(MoO_4)^{2-}$ ligands. Details of the hydrothermal synthesis, spectral characterization and structure of **1** are described in this report.

2 Results and discussion

2.1 Synthetic aspects, spectral and thermal studies

The oxidovanadium(IV) containing compound **1** was prepared by a hydrothermal reaction of molybdic acid, sodium metavanadate and 2,2′:6′,2″-terpyridine as dark green crystalline blocks. A comparison of the experimental powder pattern of a bulk sample of **1** with that of the calculated pattern (Figure S1) reveals the formation of a phase pure product. In this reaction the N-donor serves as a structure directing ligand as well as a reducing agent. The formation of a $[VO]^{2+}$ containing compounds starting from V^{5+} reactants in the presence of N-donor ligands under hydrothermal conditions is a well-known synthetic methodology in the literature [30, 32]. The presence of V^{4+} is confirmed by the characteristic ESR signal centred at g = 1.987 of a polycrystalline sample of **1** (Figure S2). The infrared (IR) and Raman spectra (Figures S3 and S4) of **1** exhibit several characteristic bands. The broad IR band centred at around 3410 cm^{-1} and the signal at 1609 cm^{-1} can be attributed to the stretching and bending vibrations respectively of the –OH moiety of lattice water. The IR spectrum also consists of peaks arising due to V–O (terminal) and various Mo–O stretching vibrations at 946, 893, 796, 725, 672, 543, 452 cm^{-1}. The intense Raman signal at 968 cm^{-1} can be assigned for a vibration of the γ-$[Mo_8O_{26}]^{4-}$ unit [33]. The TG-DTA curves of **1** exhibit an initial mass loss of 1.2% (Calcd: 1.3%) accompanied by a weak endothermic signal centered at 92 °C assignable for the loss of coordinated water (Figure S5). This is followed by an exothermic peak at 440 °C corresponding to a large mass loss of 34.5%. This value is in close agreement with the calculated value of 34.0% for loss of the organic ligand. The residual mass of 64.3% (Calcd. 65.8%) can be assigned for the formation of a phase of composition $V_2Mo_5O_{20}$.

2.2 Description of the crystal structure of 1

The title coordination polymer **1** $[(VO(terpy))_4(MoO_4)_2(Mo_8O_{26})]\cdot 2H_2O$ crystallizes in the centrosymmetric triclinic space group $P\bar{1}$. Its structure consists of a crystallographically unique γ-$(Mo_8O_{26})^{4-}$ anion located on an inversion centre, an independent tetraoxidomolybdate $(MoO_4)^{2-}$ dianion, two crystallographically unique $(VO(terpy))^{2+}$ moieties and a lattice water molecule (Figure 1). Both the unique vanadium V1 and V2 species are bonded to a terminal oxido ligand O1 and O2, respectively, and are further coordinated to a terpy ligand, whose three N atoms span the meridional sites of a $\{VN_3O_3\}$ octahedron. The geometric parameters of the two crystallographically unique terpyridine ligands bonded to V1 and V2 are in normal range (Table S1).

The first unique V^{4+} (V1) is further bonded to two oxygen atoms (O5 and O6) of $(MoO_4)^{2-}$ while the second independent V (V2) is bonded to O4 of $(MoO_4)^{2-}$ and O7 of $(Mo_8O_{26})^{4-}$ completing the $\{VN_3O_3\}$ octahedron. The terminal oxido ligands O1 and O2 make the shortest V–O bonds (Table 1). Unlike the V–O distances which range from 1.5940(17) to 2.1833(16) Å for V1 (1.5998(16) to 2.1198(16) for V2), the V–N bond distances scatter in a narrow range between 2.0643(18) and 2.149(2) Å for V1 (2.0452(18) and 2.131(2) for V2). Bond valence sum of the V–N and V–O bonds for V1 and V2 were determined using the VaList program [34]. The values of 3.77 and 3.81 for V1 and V2 reveal that the unique vanadium atoms can be formulated as V(IV). The *cis*- as well as the *trans*- O–V–N or N–V–N angles deviate from ideal values and cover a wide range (76.36(8) to 101.97(7) and 152.35(8)° to 178.54(8)° for V1; 76.83(8)° to 104.11(7)° and 151.79(8)° to 177.15(9)° for V2) indicating a distortion of the $\{VN_3O_3\}$ octahedron. The Mo–O bond lengths of the tetrahedral $(MoO_4)^{2-}$ anion range from the shortest Mo–O3 bond of 1.7159(19) to 1.8042(16) Å for Mo–O6. The binding of O6 with V1 can explain the elongation of the Mo–O6 bond. The O–Mo–O bond angles range from 107.79(7)° to 112.53(8)° indicating a slight distortion of the $\{MoO_4\}$ tetrahedron.

The tetraanionic octamolybdate $(Mo_8O_{26})^{4-}$ is well-known to exhibit polymorphism and several polymorphic modifications are well documented in the literature [35–44]. Although the α- and β-modifications are more often encountered, other polymorphic forms like γ, δ, ε etc.

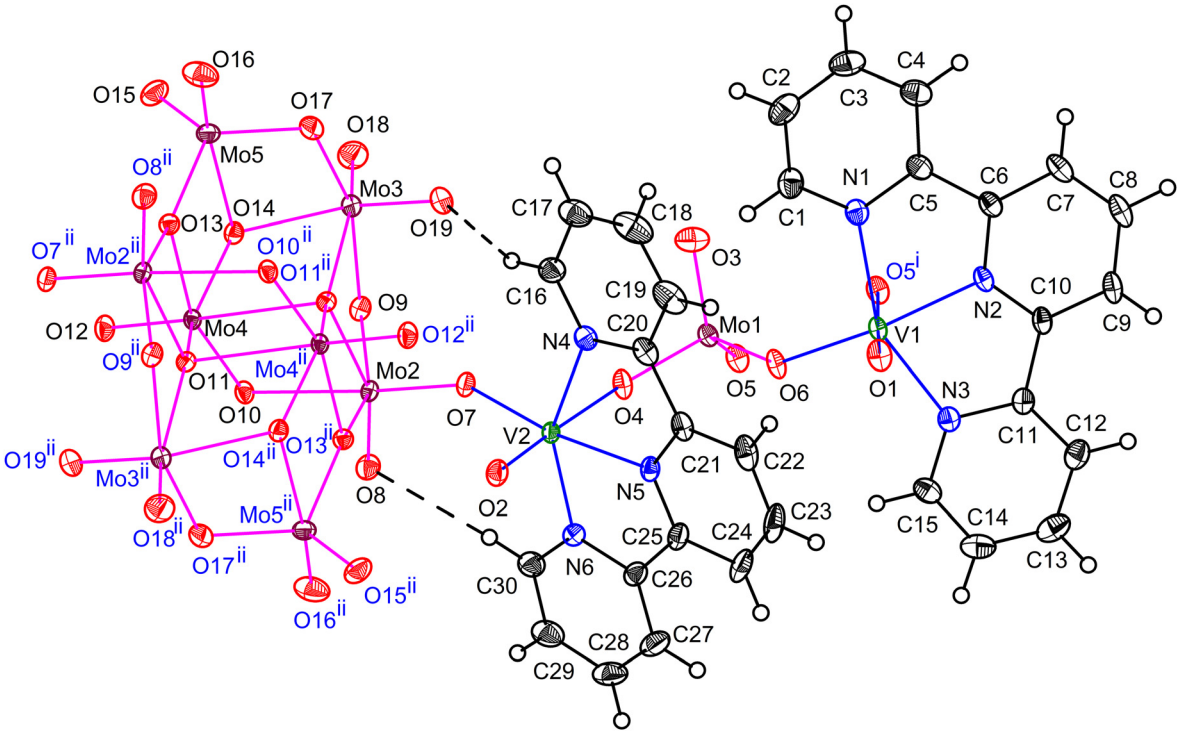

Figure 1: The asymmetric unit of **1** showing sixfold coordination around V1 and V2. Displacement ellipsoids are drawn at 30% probability level for all the non-hydrogen atoms. Intramolecular H-bonding is shown as broken lines. For clarity, symmetry generated atoms are labelled in blue. Symmetry code: (i) $-x, -y+1, -z+1$ (ii) $-x+1, -y+2, -z+2$.

are also known (Table S2). The centrosymmetric $(Mo_8O_{26})^{4-}$ unit in **1** which consists of three unique octahedrally surrounded Mo atoms (Mo2, Mo3 and Mo4) and the pentacoordinated Mo5 atom (Figure S6) is a γ-modification of $(Mo_8O_{26})^{4-}$ and the 13 unique O atoms can be classified under four types viz. i) the terminal oxido (O_t) ligands O7, O8, O12, O15, O16, O18 and O19, ii) μ_2-bridging oxido ligands O9, O10, O17 iii) μ_3-bridging O13 and O14 iv) μ_4-bridging O11. The terminal Mo–O_t bond distances range from 1.6884(16) to 1.7605(15) Å. O7 which makes the longest Mo2–O7 distance of 1.7605(15) Å has also a bond to V2, which can explain its elongation. Unlike the terminal oxygen atoms, the bridging oxido ligands exhibit longer Mo–O distances which scatter in a wider range viz. 1.7648(15)–2.2146(15) Å for μ_2-bridging ligands, and 1.8995(15)–2.3318(15) Å and 1.8973(14)–2.5049(14) Å for μ_3- and μ_4-bridging ligands respectively.

Oxidovandium(IV) compounds containing monodentate and bridging $(MoO_4)^{2-}$ ligand are well documented in the literature [30, 32]. Compound **1** is unique due to the presence of two different Mo-based ligands viz. $(MoO_4)^{2-}$ and $(Mo_8O_{26})^{4-}$. To the best of our knowledge no other V^{4+} compound is known containing coordinated $(MoO_4)^{2-}$ and $(Mo_8O_{26})^{4-}$ ligands. Zubieta and coworkers reported an example of a three-dimensional Cu(II) compound $[\{Cu_2(L_4)\}_2\{\gamma\text{-}Mo_8O_{26}\}\{MoO_4\}_2]\cdot 2H_2O$ (entry 4 in Table S2) containing two differing molybdate ligands [37].

The μ_3-bridging $(MoO_4)^{2-}$ dianion binds to two symmetry related V1 atoms via O5 and O6 and a V2 through O4 while the centrosymmetric $(Mo_8O_{26})^{4-}$ binds to V2 via O7 (Figure S7). The μ_3-bridging tridentate binding of $(MoO_4)^{2-}$ results in the formation of a $\{V_4Mo_2O_{12}\}^{4+}$ cationic unit which is composed of an eight membered heterometallic $\{Mo_2V_2O_4\}$ ring containing one of the unique V atoms (V1 in the ring) with the other unique V atom (V2) protruding as handles (Figure 2).

A pair of $\{V_4Mo_2O_{12}\}^{4+}$ units are bridged by a $(Mo_8O_{26})^{4-}$ ligand resulting in the formation of a polymeric chain which consists of alternating $\{V_4Mo_2O_{12}\}^{4+}$ cations and $(Mo_8O_{26})^{4-}$ anions (Figure 3). The H atoms attached to the carbon atoms C4, C7, C9, C14, C16, C19, C24, C27, C29 and C30 of the unique terpy ligands function as hydrogen donors while the O atoms O1 and O2 attached to V1 and V2 and the O atoms of the γ-$(Mo_8O_{26})^{4-}$ unit, viz. O8, O9, O10, O14,

Table 1: Bond lengths and angles (Å, °) of $\{VN_3O_3\}$, $(MoO_4)^{2-}$ and $(Mo_8O_{26})^{4-}$ moieties in **1**.

V1–O1	1.5940(17)	Mo1–O4	1.7637(16)	Mo3–O18	1.6892(19)
V1–O5^{i}	2.1833(16)	Mo1–O5	1.7750(16)	Mo3–O19	1.7029(18)
V1–O6	1.9674(15)	Mo1–O6	1.8042(16)	Mo4–O10	1.7648(15)
V1–N1	2.142(2)	Mo2–O7	1.7605(15)	Mo4–O11	1.8973(14)
V1–N2	2.0643(18)	Mo2–O8	1.6884(16)	Mo4–O11^{ii}	2.5049(14)
V1–N3	2.1490(2)	Mo2–O9	1.8539(15)	Mo4–O12	1.6886(15)
V2–O2	1.5998(16)	Mo2–O10	2.2146(15)	Mo4–O14	1.8995(15)
V2–O4	2.1198(16)	Mo2–O11^{ii}	2.2450(14)	Mo4–O13	2.2101(15)
V2–O7	2.0096(15)	Mo2–O13^{ii}	2.0192(14)	Mo5–O13	1.9076(15)
V2–N4	2.1231(19)	Mo3–O9	1.9724(16)	Mo5–O14	2.3318(15)
V2–N5	2.0452(18)	Mo3–O11^{ii}	2.4960(15)	Mo5–O15	1.7032(18)
V2–N6	2.131(2)	Mo3–O14	2.1297(15)	Mo5–O16	1.6949(19)
Mo1–O3	1.7159(19)	Mo3–O17	1.9819(18)	Mo5–O17	1.8579(18)
O1–V1–O6	100.44(8)	O8–Mo2–O9	104.32(8)	O11–Mo4–O13	73.39(6)
O1–V1–N2	100.17(8)	O7–Mo2–O9	101.46(7)	O14–Mo4–O13	75.28(6)
O6–V1–N2	159.39(7)	O8–Mo2–O13^{ii}	101.14(7)	O12–Mo4–O11^{ii}	175.01(7)
O1–V1–N1	94.12(9)	O7–Mo2–O13^{ii}	90.94(6)	O10–Mo4–O11^{ii}	75.15(6)
O6–V1–N1	101.90(8)	O9–Mo2–O13^{ii}	148.10(6)	O11–Mo4–O11^{ii}	79.50(6)
N2–V1–N1	76.37(8)	O8–Mo2–O10	85.89(7)	O14–Mo4–O11^{ii}	71.37(5)
O1–V1–N3	95.08(9)	O7–Mo2–O10	168.50(6)	O13–Mo4–O11^{ii}	83.38(5)
O6–V1–N3	101.97(7)	O9–Mo2–O10	82.54(6)	O16–Mo5–O15	105.15(10)
N2–V1–N3	76.36(8)	O13^{ii}–Mo2–O10	80.42(6)	O16–Mo5–O17	101.46(9)
N1–V1–N3	152.35(8)	O8–Mo2–O11^{ii}	158.66(7)	O15–Mo5–O17	112.62(9)
O1–V1–O5^{i}	178.54(8)	O7–Mo2–O11^{ii}	96.52(6)	O16–Mo5–O13	99.59(8)
O6–V1–O5^{i}	80.88(6)	O9–Mo2–O11^{ii}	78.91(6)	O15–Mo5–O13	116.32(8)
N2–V1–O5^{i}	78.51(7)	O13^{ii}–Mo2–O11^{ii}	70.48(6)	O17–Mo5–O13	118.38(7)
N1–V1–O5^{i}	84.99(7)	O10–Mo2–O11^{ii}	73.51(5)	O16–Mo5–O14	166.35(9)
N3–V1–O5^{i}	85.21(7)	O18–Mo3–O19	105.13(10)	O15–Mo5–O14	88.39(8)
O2–V2–O7	95.20(7)	O18–Mo3–O9	98.92(9)	O17–Mo5–O14	74.17(6)
O2–V2–N5	95.15(8)	O19–Mo3–O9	96.60(8)	O13–Mo5–O14	72.22(6)
O7–V2–N5	169.48(7)	O18–Mo3–O17	99.81(9)	Mo1–O4–V2	146.34(9)
O2–V2–O4	177.15(9)	O19–Mo3–O17	93.97(9)	Mo1–O5–V1^{i}	144.17(10)
O7–V2–O4	85.34(6)	O9–Mo3–O17	155.26(7)	Mo1–O6–V1	134.78(9)
N5–V2–O4	84.42(7)	O18–Mo3–O14	100.75(8)	Mo2–O7–V2	145.82(9)
O2–V2–N4	98.67(9)	O19–Mo3–O14	153.66(8)	Mo2–O9–Mo3	119.09(8)
O7–V2–N4	99.70(7)	O9–Mo3–O14	84.02(6)	Mo4–O10–Mo2	118.35(7)
N5–V2–N4	76.83(8)	O17–Mo3–O14	76.72(6)	Mo4–O11–Mo2^{ii}	108.74(6)
O4–V2–N4	83.98(7)	O18–Mo3–O11^{ii}	165.24(8)	Mo4–O11–Mo3^{ii}	158.74(7)
O2–V2–N6	94.07(9)	O19–Mo3–O11^{ii}	86.91(8)	Mo2^{ii}–O11–Mo3^{ii}	88.02(5)
O7–V2–N6	104.11(7)	O9–Mo3–O11^{ii}	70.76(5)	Mo4–O11–Mo4^{ii}	100.50(6)
N5–V2–N6	77.03(8)	O17–Mo3–O11^{ii}	87.60(6)	Mo2^{ii}–O11–Mo4^{ii}	92.12(5)
O4–V2–N6	83.09(7)	O14–Mo3–O11^{ii}	68.34(5)	Mo3^{ii}–O11–Mo4^{ii}	91.60(5)
N4–V2–N6	151.79(8)	O12–Mo4–O10	103.48(7)	Mo5–O13–Mo2^{ii}	142.53(8)
O3–Mo1–O4	109.17(10)	O12–Mo4–O11	105.48(7)	Mo5–O13–Mo4	108.46(6)
O3–Mo1–O5	109.80(9)	O10–Mo4–O11	99.25(7)	Mo2^{ii}–O13–Mo4	105.69(6)
O4–Mo1–O5	107.93(8)	O12–Mo4–O14	104.37(7)	Mo4–O14–Mo3	125.60(7)
O3–Mo1–O6	109.54(9)	O10–Mo4–O14	100.23(7)	Mo4–O14–Mo5	104.03(6)
O4–Mo1–O6	107.79(7)	O11–Mo4–O14	139.13(6)	Mo3–O14–Mo5	93.44(6)
O5–Mo1–O6	112.53(8)	O12–Mo4–O13	98.19(7)	Mo5–O17–Mo3	115.67(8)
O8–Mo2–O7	103.33(8)	O10–Mo4–O13	158.30(6)		

Symmetry transformations used to generate equivalent atoms: Symmetry code: i) $-x, -y + 1, -z + 1$; ii) $-x + 1, -y + 2, -z + 2$.

O15, O17 and O19 function as hydrogen acceptors resulting in a total of eleven C–H···O bonds (Table S3) of which two are intramolecular. The intermolecular C–H···O bonds serve to link parallel polymeric chains. The difficulty to locate the H atoms attached to the lattice water precludes a description of the O–H···O interactions.

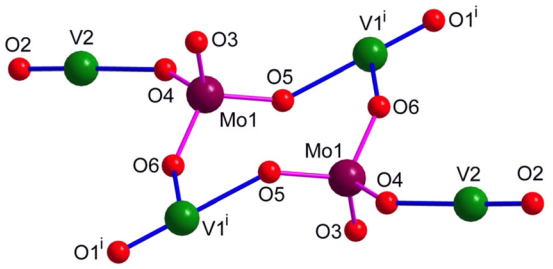

Figure 2: The $\{V_4Mo_2O_{12}\}^{4+}$ cationic unit made up of an eight-membered heterometallic $\{Mo_2V_2O_4\}$ ring with protruding oxidovanadium handles. The terpy ligands around V1 and V2 are not shown. Symmetry code i) $-x, -y + 1, -z + 1$.

3 Experimental

3.1 Materials and methods

All chemicals were used as received from commercial sources without any further purification. Infrared (IR) spectra of the solid samples diluted with KBr were recorded on a Shimadzu (IR Prestige-21) FT-IR spectrometer in the range 4000–400 cm^{-1} at a resolution of 4 cm^{-1}. The Raman spectrum was recorded using a Labram HR Evolution Raman Spectrometer HORIBA Scientific at 785 nm laser radiation for excitation and laser power set to 5%. An ESR spectrum was recorded in a Jeol (JES, FA200) spectrometer using a microwave frequency of 9.5 GHz and modulation frequency of 100 kHz at Sophisticated Analytical Instruments Facility (SAIF), IIT-Madras. The elemental analysis (C, H and N) was performed on an Elementar Variomicro Cube CHNS Analyser. TG-DTA experiment was performed in air at the heating rate of 5 K/min in the temperature range of 30–700 °C on STA-409 PC simultaneous thermal analyser from Netzsch in an alumina crucible. Powder X-ray diffraction (PXRD) pattern was recorded on a Rigaku Smartlab powder diffractometer using Cu-*Kα* radiation. For single crystal structure determination, X-ray intensity data was collected on a Bruker D8 Quest Eco X-ray diffractometer, using graphite-monochromated Mo-Kα radiation. The structure was solved with Direct Methods using Shelxs-97 [45] and refinement was carried out against F^2 using Shelxl-2016 [45]. All non-hydrogen atoms were refined anisotropically. The H atoms bonded to the aromatic carbons were located in difference Fourier maps but were positioned with idealized geometry and refined isotropically with $U_{iso}(H) = 1.2\ U_{eq}(C)$ using a riding model. The hydrogen atoms attached to the lattice water O1W could not be located. Technical details of data acquisition and selected refinement results for **1** are given in Table 2.

4 Synthesis of $[(VO(terpy))_4(MoO_4)_2(Mo_8O_{26})]$ 1

Compound **1** was synthesized under hydrothermal conditions in a steel autoclave with Teflon container (volume 25 mL). Sodium metavanadate (0.046 g, 0.38 mmol), 2,2′:6′,2″-terpyridine (0.116 g, 0.497 mmol) and molybdic

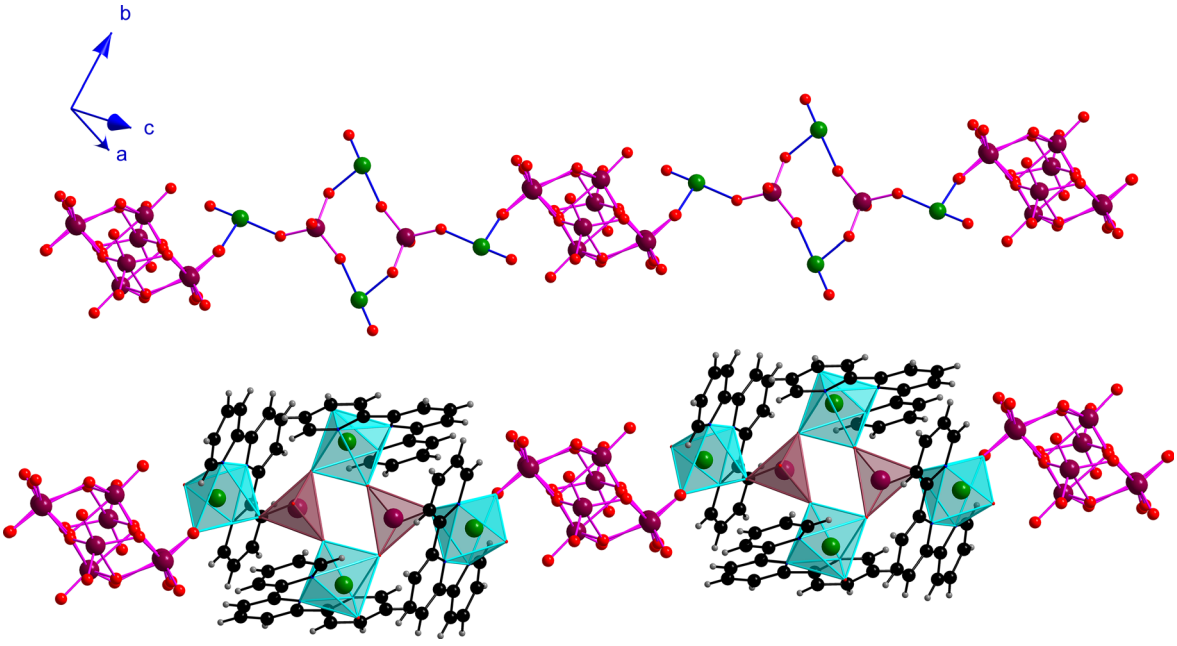

Figure 3: A portion of an infinite chain showing alternating $(Mo_8O_{26})^{4-}$ anions and $\{V_4Mo_2O_{12}\}^{4+}$ cations. The tridentate terpy ligands on the unique V atoms are not shown (**top**). Same arrangement after inclusion of the terpy ligands. The $\{VO_3N_3\}$ octahedra and $(MoO_4)^{2-}$ tetrahedra are shown in polyhedral format (**bottom**).

Table 2: Selected refinement results for $[(VO(terpy))_4(MoO_4)_2(Mo_8O_{26})]\cdot 2H_2O$ **1**.

Refinement result	Compound 1
Empirical formula	$C_{30}\ H_{24}\ Mo_5\ N_6\ O_{20}\ V_2$
Formula weight (g mol^{-1})	1370.14
Temperature (K)	296(2)
Wavelength (Å)	0.71073
Crystal system	Triclinic
Space group	$P\bar{1}$
Unit cell dimensions	
a (Å)	11.4507(16)
b (Å)	11.8541(17)
c (Å)	14.675(2)
α (°)	92.023(4)
β (°)	98.321(4)
γ (°)	91.804(4)
Volume (Å^3)	1968.4(5)
Z	2
D_{calc} (g cm^{-3})	2.31
Absorption coefficient (mm^{-1})	2.1
F(000)	1320
Crystal size (mm^3)	0.24 × 0.16 × 0.14
θ range for data collection (°)	2.53–28.31
Limiting indices	$-15 \le h \le 15$
	$-15 \le k \le 15$
	$-19 \le l \le 19$
Reflections collected/unique	66,874/9787
	[R(int) = 0.0290]
Completeness θ = 25.242°	99.9
Refinement method	Full-matrix least-squares on F^2
Data/restraints/parameters	9787/0/568
Goodness of fit on F^2	1.104
Final R indices [$I > 2\sigma(I)$]	$R1$ = 0.0198
	w$R2$ = 0.0480
R indices (all data)	$R1$ = 0.0238
	w$R2$ = 0.0507
Largest diff. peak and hole (e Å^{-3})	0.67 and −0.73
Bond valence sum	V1 = 3.77; V2 = 3.81
CCDC Deposition No	2131584

acid (0.094 g, 0.58 mmol) were taken in water (~8 mL) and acetic acid (99.0%) was added to make the pH ~ 3 and the reaction mixture was heated at 200 °C for 68 h. The green reaction mixture was filtered and washed with water to obtain dark green crystalline blocks of **1** (Yield = 0.092 g, 35%).

Analytical data (%) Calcd.: C, 26.29; N, 6.13; H, 1.77. Found: C, 26.97; N, 6.31; H, 1.83.

IR data (KBr, cm^{-1}): 3410(br), 3084–2928(m), 1609(s), 1446(s), 1400(m), 1322(m), 1244(m), 1166(m), 1108(m), 1050(m), 946(s), 893(vs), 796(s), 725(s), 672(s), 543(m), 452(m).

Raman data (cm^{-1}): 1047, 968(vs), 881, 825.

5 Supporting information

Deposition number CCDC 2131584 (**1**), contains the supplementary crystallographic data for this paper. These data are provided free of charge by the joint Cambridge Crystallographic Data Centre and Fachinformationszentrum Karlsruhe Access Structures service www.ccdc.cam.ac.uk/structures. Supplementary Data (Figs. S1–S7) and Tables S1–S3 associated with this article are available in electronic form.

Acknowledgments: The authors thank the Department of Science and Technology (DST), New Delhi, for the sanction of a Bruker Eco D8 Quest instrument under the FIST program. Miss Nikita N. Harmalkar acknowledges Research Studentship from Goa University.

Author contributions: All the authors have accepted responsibility for the entire content of this submitted manuscript and approved submission.

Research funding: SND thanks Council of Scientific and Industrial Research (CSIR), New Delhi, India (No. 01(2923)/18/EMR-II) for funding.

Conflict of interest statement: The authors declare no conflicts of interest regarding this article.

References

1. Pope M. T., Müller A. *Polyoxometalate Chemistry from Topology via Self-Assembly to Applications*; Kluver Academic Publishers: Amsterdam, 2002.
2. Pope M. T., Müller A. Polyoxometalate chemistry: an old field with new dimensions in several disciplines. *Angew. Chem, Int. Ed. Engl.* 1991, *30*, 34–48.
3. Dolbecq A., Dumas E., Mayer C. R., Mialane P. Hybrid organic-inorganic polyoxometalate compounds: from structural diversity to applications. *Chem. Rev.* 2010, *110*, 6009–6048.
4. Xiao L.-N., Zhao C.-X., Shi X.-M., Zhang H., Wu W., Cui X.-B. Three new compounds based on similar molybdenum-vanadium clusters and several types of copper complexes. *CrystEngComm* 2018, *20*, 969–977.
5. Aureliano M., Crans D. C. Decavanadate $(V_{10}O_{28})^{6-}$ and oxovanadates: oxometalates with many biological activities. *J. Inorg. Biochem.* 2009, *103*, 536–546.
6. Bijelic A., Aureliano M., Rompel A. The antibacterial activity of polyoxometalates: structures, antibiotic effects and future perspectives. *Chem. Commun.* 2018, *54*, 1153–1169.
7. Cao Y., Chen Q., Shen C., He L. Polyoxometalate-based catalysts for CO_2 conversion. *Molecules* 2019, *24*, 2069–2095.
8. Zhou Y., Chen G., Long Z., Wang J. Recent advances in polyoxometalate-based heterogeneous catalytic materials for liquid-Phase organic transformations. *RSC Adv.* 2014, *4*, 42092–42113.
9. Lang X., Chen X., Zhao J. Heterogeneous visible light photocatalysis for selective organic transformations. *Chem. Soc. Rev.* 2014, *43*, 473–486.

10. Wang D., Liu L., Jiang J., Chen L., Zhao J. Polyoxometalate-based composite materials in electrochemistry: state-of-the-art progress and future outlook. *Nanoscale* 2020, *12*, 5705–5718.
11. Kögerler P., Tsukerblat B., Müller A. Structure-related frustrated magnetism of nanosized polyoxometalates: aesthetics and properties in harmony. *Dalton Trans.* 2020, *39*, 21–36.
12. Liang Y., Li Y., Wang H., Dai H. Strongly coupled inorganic/nanocarbon hybrid materials for advanced electrocatalysis. *J. Am. Chem. Soc.* 2013, *135*, 2013–2036.
13. Wang S.-S., Yang G.-Y. Recent advances in polyoxometalate-catalyzed reactions. *Chem. Rev.* 2015, *115*, 4893–4962.
14. Anyushin A. V., Kondinski A., Parac-Vogt T. N. Hybrid polyoxometalates as post-functionalization platforms: from fundamentals to emerging applications. *Chem. Soc. Rev.* 2020, *49*, 382–432.
15. Monakhov K. Y., Bensch W., Kögerler P. Semimetal-functionalised polyoxovanadates. *Chem. Soc. Rev.* 2015, *44*, 8443–8483.
16. Mahnke L. K., Kondinski A., Warzok U., Näther C., van Leusen J., Schalley C. A., Monakhov K. Y., Kögerler P., Bensch W. Configurational isomerism in polyoxovanadates. *Angew. Chem. Int. Ed.* 2018, *57*, 2972–2975.
17. Mahnke L. K., Stehlíková G., Synnatschke K., Backes C., Näther C., Bensch W. An exotic layered compound consisting of interconnected arsenato-polyoxovanadate clusters: thermal and magnetic properties and liquid phase exfoliation. *ChemNanoMat* 2021, *7*, 78–84.
18. Aureliano M. Decavanadate: a journey in a search of a role. *Dalton Trans.* 2009, 9093–9100; https://doi.org/10.1039/B907581J.
19. Day V. W., Klemperer W. G., Maltbie D. J. Where are the protons in $H_3V_{10}O_{28}^{3-}$? *J. Am. Chem. Soc.* 1987, *109*, 2991–3002.
20. Evans H. T., Jr. The molecular structure of the isopoly complex ion, decavanadate $(V_{10}O_{28})^{6-}$. *Inorg. Chem.* 1966, *5*, 967–977.
21. Groom C. R., Bruno I. J., Lightfoot M. P., Ward S. C. The Cambridge structural database. *Acta Crystallogr.* 2016, *B72*, 171–179.
22. Wutkowski A., Srinivasan B. R., Naik A. R., Schütt C., Näther C., Bensch W. Synthesis, structure, and photochemistry of an organic heptamolybdate-monomolybdate. *Eur. J. Inorg. Chem.* 2011, 2254–2263; https://doi.org/10.1002/ejic.201001154.
23. Srinivasan B. R., Kundaikar S. A., Morajkar S. M., Näther C., Bensch W. Synthesis, crystal structure and properties of hepta(ammonium) penta(1H-imidazol-3-ium) paratungstate B tetrahydrate. *J. Coord. Chem.* 2021, *74*, 2239–2252.
24. Pope M. T., Dale B. W. Isopoly-vanadates, -niobates, and -tantalates. *Q. Rev. Chem. Soc.* 1968, *22*, 527–548.
25. Higami T., Hashimoto M., Okeya S. $[Ni(H_2O)_6]_2[Na(H_2O)_3]_2[V_{10}O_{28}]\cdot 4H_2O$, bis(nickel hexahydrate) bis(sodium trihydrate) decavanadate tetrahydrate. *Acta Crystallogr.* 2002, *C58*, i144–i146.
26. Iida A., Ozeki T. $Cu_3V_{10}O_{28}\cdot 24H_2O$ and $CuNa_4V_{10}O_{28}\cdot 23H_2O$. *Acta Crystallogr.* 2003, *C59*, i41–i44.
27. Iida A., Ozeki T. $Mg_2Na_2V_{10}O_{28}\cdot 20H_2O$ and $Mg_3V_{10}O_{28}\cdot 28H_2O$. *Acta Crystallogr.* 2004, *C60*, i43–i46.
28. Putrevu N. R., Doedens R. J., Khan M. I. Decavanadate with a novel coordination complex: synthesis and characterization of $(NH_4)_2[Ni(H_2O)_5(NH_3)]_2(V_{10}O_{28})\cdot 4H_2O$. *Inorg. Chem. Commun.* 2013, *38*, 5–7.
29. Johnson G. K., Schlemper E. O. Existence and structure of the molecular ion 18-vanadate(IV). *J. Am. Chem. Soc.* 1978, *100*, 3645–3646.
30. Rasmussen M., Näther C., Bismayer U., Bensch W. Small non-polar complexes exhibiting significant piezoelectric properties: solvothermal synthesis and crystal structures of $MO_5V(tren)\cdot H_2O$ (M = Mo and W; tren = tris(2-aminoethyl)amine). *J. Solid State Chem.* 2012, *195*, 108–114.
31. Finn R. C., Zubieta J. Solid state coordination chemistry: the hydrothermal synthesis and structure of a bimetallic oxide incorporating 2,2′:6′,2″-terpyridine (terpy), $[\{VO(terpy)\}MoO_4]$. *Inorg. Chim. Acta* 2002, *332*, 186–190.
32. Khan M. I., Giri S., Ayesh S., Doedens R. J. Synthesis and characterization of a new hybrid chain derived from oxovanadyl and molybdate moieties $[V^{IV}O(\mu_3\text{-}MoO_4)(2,2'\text{-bpy})]$: topological equivalence of $\{MoO_4\}$ and $\{SO_4\}$ motifs. *Inorg. Chem. Commun.* 2004, *7*, 721–724.
33. Himeno S., Niiya H., Ueda T. Raman studies on the identification of isopolymolybdates in aqueous solution. *Bull. Chem. Soc. Jpn.* 1997, *70*, 631–637.
34. Wills A. S. VaList program. http://ccp14.cryst.bbk.ac.uk/solution/bond_valence/index.html.
35. Yang W., Lu C., Zhuang H. Hydrothermal synthesis and structures of three new copper complexes: $[\{Cu(2,2'\text{-bipy}\}_2(\beta\text{-}Mo_8O_{26})]$, $[\{Cu(Py)_3\}_2\{Cu(Py)_2\}_2(\alpha\text{-}Mo_8O_{26})]$ and $[\{Cu(Py)_2\}_4]\text{-}[(SO_4)(Mo_{12}O_{36})]$. *J. Chem. Soc., Dalton Trans.* 2002, 2879–2884; https://doi.org/10.1039/B111480H.
36. Ying J., Sun C., Jin L., Tian A., Wang X. Five compounds based on $[TeMo_6O_{24}]^{6-}$ and $[\beta\text{-}Mo_8O_{26}]^{4-}$ anions synthesized by using different symmetrical and asymmetric N-donor ligands. *CrystEngComm* 2021, *23*, 5385–5396.
37. Bartholomä M., Jones S., Zubieta J. Construction of bimetallic oxide materials from molybdate building blocks and copper-ligand tethers with flexible spaces: structures of the two-dimensional $[\{Cu_2(L_4)(H_2O)_2\}Mo_8O_{26}(H_2O)_2]$ and of the three-dimensional $[\{Cu_2(L_4)\}_2(Mo_8O_{26})(MoO_4)_2]$ (L_4 = N^1, N^1, N^4, N^4-tetrakis(pyridine-2-ylmethyl)butane-1,4-diamine). *Inorg. Chem. Commun* 2011, *14*, 107–110.
38. Meng J.-X., Lu Y., Li Y.-G., Fu H., Wang E.-B. Base-directed self-assembly of octamolybdate-based frameworks decorated by flexible N-containing ligands. *Cryst. Growth Des.* 2009, *9*, 4116–4126.
39. Hagrman D., Zubeita C., Rose D. J., Zubieta J., Haushalter R. C. Composite solids constructed from one-dimensional coordination polymer matrices and molybdenum oxide subunits: polyoxomolybdate clusters within $[\{Cu(4,4'\text{-bpy})\}_4Mo_8O_{26}]$ and $[\{Ni(H_2O)_2(4,4'\text{-bpy})_2\}_2Mo_8O_{26}]$ and one-dimensional oxide chains in $[\{Cu(4,4'\text{-bpy})\}_4Mo_{15}O_{47}]\cdot 8H_2O$. *Angew. Chem. Int. Ed. Engl.* 1997, *36*, 873–876.
40. Allis D. G., Rarig R. S., Burkholder E., Zubieta J. A three-dimensional bimetallic oxide constructed from octamolybdate clusters and copper-ligand cation polymer subunits. A comment on the stability of the octamolybdate isomers. *J. Mol. Struct.* 2004, *688*, 11–31.
41. Rarig R. S., Bewley L., Burkholder E., Zubieta J. Organic-inorganic hybrid materials of the copper molybdate family. Syntheses and structures of $[Cu(tpa)Mo_2O_7]$, $[Cu(Me_2bpy)Mo_2O_7]$ and $[Cu(t\text{-}Bu_2bpy)Mo_4O_{13}]$ (tpa = tri-2-pyridylamine, Me_2bpy = 5,5′-dimethyl-2,2′-bipyridine, $t\text{-}Bu_2bpy$ = 4,4′-di-tert-butyl-2,2′-bipyridine). *Indian J. Chem.* 2003, *42A*, 2235–2243.
42. Lan Y.-Q., Li S.-L., Wang X.-L., Shao K.-Z., Su Z.-M., Wang E.-B. Supramolecular isomerism with polythreaded topology based on $[Mo_8O_{26}]^{4-}$ isomers. *Inorg. Chem.* 2008, *47*, 529–534.

43. Yue Z.-C., Du H.-J., Niu Y.-Y., Jin G.-X. An unprecedented ι-type octamolybdate: $[TbI_1]_2[(\beta\text{-}Mo_8O_{26})_{0.5}(\iota\text{-}Mo_8O_{26})]$ directed by a new tricationic template. *CrystEngComm* 2013, *15*, 9844–9848.
44. Sarr B., Diop C. A. K., Melin F., Sidibe M., Hellwig P., Michaud F., Maury F., Senocq F., Mbaye A., Rousselin Y. Non-Hydrothermal synthesis and structure determination of two new β-octamolybdate (VI) stabilized with dialkylammonium counterions. *J. Mol. Struct.* 2018, *1170*, 44–50.
45. Sheldrick G. M. Crystal structure refinement with Shelxl. *Acta Crystallogr*. 2015, *C71*, 3–8.